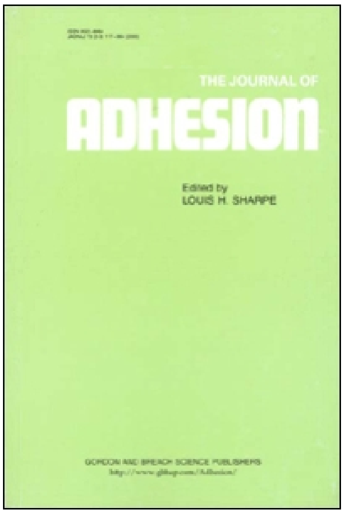

The Journal of Adhesion
Publication details, including instructions for authors and subscription information:
http://www.informaworld.com/smpp/title~content=t713453635

A Comparison of Numerous Lap Joint Theories for Adhesively Bonded Joints

William C. Carpenter[a]
[a] Department of Civil Engineering, University of South Florida, Tampa, Florida, U.S.A.

To cite this Article Carpenter, William C.(1991) 'A Comparison of Numerous Lap Joint Theories for Adhesively Bonded Joints', The Journal of Adhesion, 35: 1, 55 — 73
To link to this Article: DOI: 10.1080/00218469108030435
URL: http://dx.doi.org/10.1080/00218469108030435

J. Adhesion, 1991, Vol. 35, pp. 55–73
Reprints available directly from the publisher
Photocopying permitted by license only

Printed in the United Kingdom

A Comparison of Numerous Lap Joint Theories for Adhesively Bonded Joints

WILLIAM C. CARPENTER

Department of Civil Engineering, University of South Florida, Tampa, Florida 33620, U.S.A.

(Received December 21, 1990; in final form April 9, 1991)

Numerous authors have investigated the state of stress in the adhesive of adhesively bonded joints. They have made various assumptions concerning the behavior of the adhesive and adherends to yield tractable differential equations which remove the stress singularities which occur at the edges of the bi-material interfaces. By examining several test problems, this paper investigates the effect of these assumptions on predicted adhesive stress. It was found that predicted maximum adhesive shear stress is insensitive to underlying assumptions and that maximum adhesive peel stress is relatively unaffected by most assumptions except that neglecting shear deformation of the adherends can affect results by as much as 30%. Peel stresses from the well known theory of Goland and Reissner which neglects shear deformation of the adherends and makes several inconsistent assumptions vary as much as 30% from stresses from a consistent lap joint theory which considers shear deformation of the adherends. However, in most cases the effects of the inconsistencies cancel the effects of neglecting the shear deformation of the adherends and the variation is less than 15%. This paper points out that finite element analyses of bonded joints where one layer of 4 node isoparametric elements are used to model the adhesive give results very close to those from consistent lap joint theories.

KEY WORDS Lap joint; bonded connection; simplifying assumptions; adhesive stress; finite element analysis; shear deformation.

INTRODUCTION

Lap joint theories predict the state of stress in the thin adhesive which bonds the adherend plates. In their classic paper, Goland and Reissner presented the first modern lap joint theory.[1] Subsequently, numerous authors have proposed theories which have improved upon Goland and Reissner's basic formulation.[2–17] The common feature of all these theories is that simplifying assumptions are made concerning the behavior of the adherends and of the adhesive. These assumptions remove the stress singularities which occur at the edges of the interfaces of the adhesive and the adherends[18] and yield tractable differential equations which can be solved to yield the stresses in the adhesive. Maximum adhesive stresses from these solutions can then be used in joint design. The numerous authors who have used this approach in analyzing adhesively bonded joints have arrived at their basic differential equations by making varying simplifying assumptions. The manner in which these assumptions affect predicted adhesive stress is the topic of this paper.

The effect of a given assumption on predicted adhesive stress is difficult to determine with a differential equation approach. However, Carpenter and Barsoum[19] recently presented special adhesive finite elements which can be used to model the adhesive while plate or beam elements can be used to model the adherends. With these adhesive elements, control parameters are used to specify which assumptions are to be considered. It has been shown that results using this finite element approach converge to those of the lap joint theory having the same set of underlying assumptions.[19] By examining the effect of control parameters on adhesive stress, the importance of any given assumption associated with a lap joint theory can be ascertained.

In this paper, the common assumptions found in most lap joint theories are first discussed. Test problems are then described and the effect on predicted maximum adhesive stress of various assumptions is then investigated.

COMMONLY USED ASSUMPTIONS

The following is a description of common assumptions used in developing lap joint theories. In this paper, a set of control parameters [α_1, α_2, α_3, α_4, α_5, α_6, IFIN, and IPLANE] are used to prescribe what assumptions are currently being considered. These control parameters are nothing more than switches that can be turned on, off, or set to certain values, to effect a given assumption. The significance of these control parameters is next discussed.

Displacement Assumption and the Strain-Displacement Equations

Examine the lap joint of Figure 1. Let u be the displacement in the adhesive in the x direction and w be the displacement in the z direction. Most lap joint theories assume that the displacements in the adhesive vary thus

$$u(x,z) = (c_1 + c_2 z) f_1(x) \qquad (1)$$
$$w(x,z) = (c_3 + c_4 z) f_2(x)$$

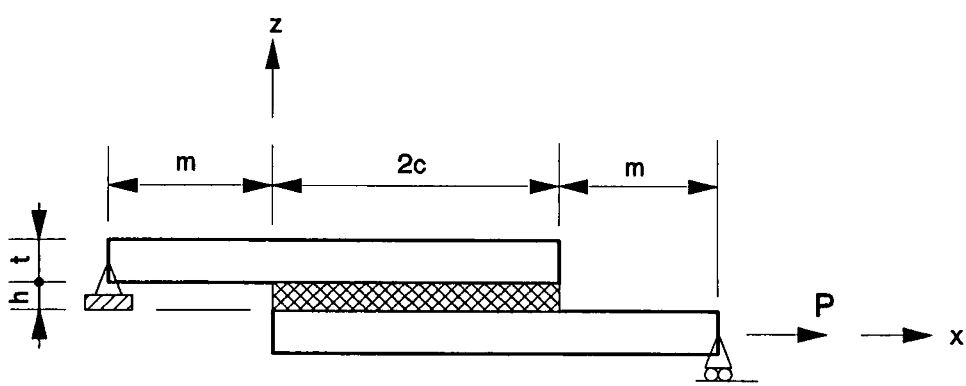

FIGURE 1 Lap joint

where c_1, c_2, c_3, and c_4 are constants and $f_1(x)$ and $f_2(x)$ are some function of x.

The strain-displacement equations for the adhesive are

$$\begin{aligned}\epsilon_x &= \frac{\partial u}{\partial x}\\ \epsilon_z &= \frac{\partial w}{\partial z}\\ \gamma_{xz} &= \frac{\partial u}{\partial z} + \alpha_1 \frac{\partial w}{\partial x}\end{aligned} \tag{2}$$

where α_1 is a control parameter which must be 1 if the complete shear strain-displacement equation is used but which is taken to be 0 by some authors.

Entering equation (1) into equation (2) gives

$$\begin{aligned}&\epsilon_x = (c_1 + \alpha_2 c_2 z) f_1'(x), \qquad \epsilon_z = c_4 f_2(x)\\ &\gamma_{xz} = c_2 f_1(x) + \alpha_1 (c_3 + \alpha_2 c_4 z) f_2'(x)\end{aligned} \tag{3}$$

where a prime denotes differentiation with respect to x and where $\alpha_2 = 1$ if no terms in the strain expressions are being neglected. The parameter α_2 can be set to zero to force the state of stress and strain in the adhesive to be constant through the thickness of the adhesive.

Authors such as Goland and Reissner[1] and Delale and Erdogan[14] use an incomplete shear strain-displacement assumption and thus take $\alpha_1 = 0$ which gives a constant shear strain through the thickness of the adhesive, as can be seen from equation (3). Authors such as Ojalvo and Eidinoff,[12] on the other hand, take $\alpha_1 = 1$ which permits the adhesive shear strain to vary through the thickness of the adhesive. Authors such as Delale and Erdogan[14] assume that strain does not vary through the thickness of the adhesive and thus take $\alpha_2 = 0$.

Shear Deformation of the Adherend

With lap joint theories, the adherends are treated as beams or plates. All modern lap joint theories consider bending and axial deformation of the adherends. Some consider shear deformation of the adherends as well, while others neglect shear deformation. In this paper, the parameter α_3 controls whether shear deformation is considered or not. If $\alpha_3 = 1$, shear deformation is considered and if $\alpha_3 \doteq 0$, shear deformation is neglected.

Finite element modeling of the adherend can be accomplished using a beam type element as shown in Figure 2. Let

$$\{\overline{P_b}\} = \begin{Bmatrix} \overline{X_1} \\ \overline{Z_1} \\ \overline{M_1} \\ \overline{X_2} \\ \overline{Z_2} \\ \overline{M_2} \end{Bmatrix}, \qquad \{\overline{\delta_b}\} = \begin{Bmatrix} \overline{u_1} \\ \overline{w_1} \\ \overline{\theta_1} \\ \overline{u_2} \\ \overline{w_2} \\ \overline{\theta_2} \end{Bmatrix} \tag{4}$$

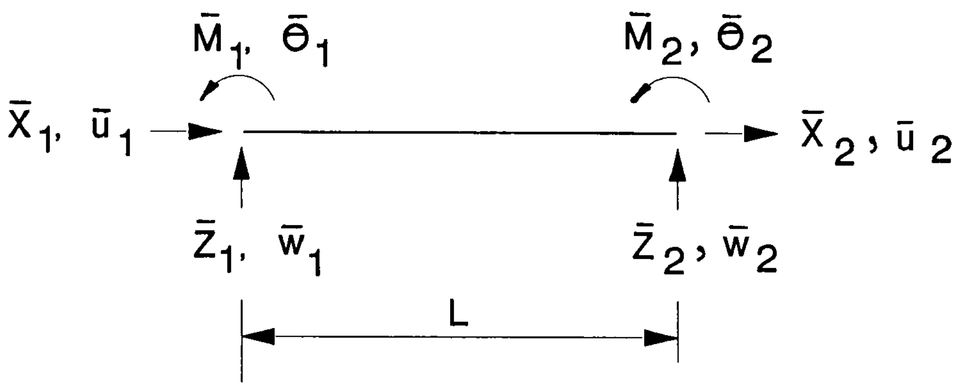

FIGURE 2 Beam type element

Then

$$\{\overline{P_b}\} = [\overline{k_b}]\{\overline{\delta_b}\} \tag{5}$$

where[20]

$$[\overline{k_b}] = \begin{bmatrix} \overline{c_1} & 0 & 0 & -\overline{c_1} & 0 & 0 \\ 0 & \overline{c_2} & \overline{c_3} & 0 & -\overline{c_2} & \overline{c_3} \\ 0 & \overline{c_3} & \overline{c_4} & 0 & -\overline{c_3} & \overline{c_5} \\ -\overline{c_1} & 0 & 0 & \overline{c_1} & 0 & 0 \\ 0 & -\overline{c_2} & -\overline{c_3} & 0 & \overline{c_2} & -\overline{c_3} \\ 0 & \overline{c_3} & \overline{c_5} & 0 & -\overline{c_3} & \overline{c_4} \end{bmatrix} \tag{6}$$

E $=$ the modulus of elasticity of the adherends,
ν $=$ Poisson's ratio of the adherends,
I $=$ moment of inertia of the adherends under plane stress conditions,
A $=$ area of the adherends under plane stress conditions,
I* $=$ I for plane stress
$= I/(1-\nu^2)$ for plane strain,
A* $=$ A for plane stress
$= \alpha_6 A/(1-\nu^2)$ for plane strain,
α_6 $=1$ for a consistent plane strain assumption for the adherends
$=$ other value for inconsistent assumptions as discussed below,
A_e $=$ the effective area in shear,[20]
α_3 $=1$ if shear deformation of the adherends is considered
$=0$ if shear deformation neglected,

$$\overline{c_1} = \frac{A^*E}{L}, \quad \overline{c_2} = \frac{12EI^*}{L^3(1+\phi)}, \quad \overline{c_3} = \frac{6EI^*}{L^2(1+\phi)}$$
$$\overline{c_4} = \frac{(4+\phi)EI^*}{L(1+\phi)}, \quad \overline{c_5} = \frac{(2-\phi)EI^*}{L(1+\phi)}, \quad \phi = \frac{12EI^*\alpha_3}{GA_eL^3} \tag{7}$$

For rectangular shaped adherends of unit width

$$A=t, \qquad I=\frac{1}{12}t^3, \qquad A_e=\frac{5}{6}t \tag{8}$$

where t is the thickness of the adherend.

Inconsistent Plane Stress—Plane Strain Assumption for the Adherends

In earlier lap joint theories such as that of Goland and Reissner,[1] the adherends were taken to be in plane strain when considering bending but were taken to be in plane stress when considering axial forces. To be consistent, for plane stress

$$I^*=I, \qquad A^*=A \tag{9}$$

and for plane strain

$$I^*=\frac{I}{1-\nu^2} \quad \mathit{and} \quad A^*=\frac{\alpha_6 A}{1-\nu^2},\ \alpha_6=1 \tag{10}$$

Goland and Reissner[1] used

$$I^*=\frac{I}{1-\nu^2} \quad \mathit{and} \quad A^*=A \tag{11}$$

which corresponds to using in equation (10)

$$\alpha_6=1-\nu^2 \tag{12}$$

Stress-Strain Equations for the Adhesive

The bonded lap joint is assumed to be elastic and is assumed to be under either plane stress or plane strain conditions. A control parameter IPLANE is used in this paper to specify which condition is being considered. If IPLANE = 0, plane stress is assumed and if IPLANE = 1, plane strain is assumed.

Adhesive stress and strain are related thus

$$\begin{Bmatrix} \sigma_z \\ \sigma_x \\ \tau_{xz} \end{Bmatrix} = [\sigma] = [D] \begin{Bmatrix} \epsilon_z \\ \epsilon_x \\ \gamma_{xz} \end{Bmatrix} \tag{13}$$

where for plane stress (IPLANE = 0)

$$[D]=\frac{E_a}{1-\nu_a^2}\begin{bmatrix} \alpha_5 & \alpha_4\nu_a & 0 \\ \alpha_4\nu_a & \alpha_4 & 0 \\ 0 & 0 & \frac{1-\nu_a}{2} \end{bmatrix} \tag{14}$$

and where for plane strain (IPLANE = 1)

$$[D]=\frac{E_a(1-\nu_a)}{(1+\nu_a)(1-2\nu_a)}\begin{bmatrix}\alpha_5 & \frac{\alpha_4\nu_a}{1-\nu_a} & 0\\ \frac{\alpha_4\nu_a}{1-\nu_a} & \alpha_4 & 0\\ 0 & 0 & \frac{1-2\nu_a}{2(1-\nu_a)}\end{bmatrix} \tag{15}$$

Goland and Reissner[1] assumed the following stress-strain relationship for the adhesive

$$\sigma_z = E_a\epsilon_z \tag{16}$$

To model this violation of the stress-strain equations one should take for plane stress

$$\alpha_5 = 1-\nu_a^2 \; and \; \alpha_4 = 0 \tag{17}$$

or for plane strain

$$\alpha_5 = \frac{(1+\nu_a)(1-2\nu_a)}{(1-\nu_a)} \; and \; \alpha_4 = 0 \tag{18}$$

Zero Adhesive Thickness Assumption

In theories which consider that the stress in the adhesive is constant through its thickness, the deformation characteristics of the adhesive are defined by the quantities E_a/h and G_a/h and not by the parameters E_a, G_a, and h themselves. Thus, it is possible to treat the adhesive as having zero thickness with properties defined by E_a/h and G_a/h. Goland and Reissner[1] and Delale and Erdogan[14] treat the adhesive in this way. This situation is referred to in this paper as the zero adhesive thickness assumption and in this paper this assumption is effected by setting the control parameter IFIN to 0. In cases where the adhesive is treated as having a finite thickness, such as with the theory of Ojalvo and Eidinoff,[14] the situation is referred to as the finite adhesive thickness assumption and IFIN is set to 1.

Table I summarizes the assumptions that are examined in this paper.

EXAMPLE 1

In this investigation, the lap joint of Figure 1 with m = 0 was considered. Particulars of the lap joint are given in Table II. The lap joint was subjected to the following load cases:

1. Membrane-Shear loading,
2. Membrane-Bending loading,
3. Shear loading, and
4. Bending loading.

These loading cases are shown in Figure 3. Reference 14 investigated cases 1, 3, and 4.

TABLE I
Control parameters

Parameter	Significance
IPLANE	=1 for plane strain =0 for plane stress
IFIN	=0 for zero adhesive thickness assumption =1 for finite adhesive thickness assumption
α_1	=0 for incomplete shear-strain displacement assumption for the adhesive =1 for complete shear-strain displacement assumption for the adhesive
α_2	=0 if adhesive strain does not vary with z =1 if adhesive strain varies linearly with z
α_3	=0 if shear deformation of the adherends is not considered =1 if shear deformation is considered
α_4	=0 if certain terms in the stress-strain equations for the adhesive are neglected =1 if those terms are not neglected
α_5	=1 if the consistent stress-strain equations for the adhesive are considered = other value if inconsistent equations used
α_6	=1 if consistent plane strain assumption for the adherends used = other value if inconsistent assumption used

TABLE II
Properties of the configuration

Parameter	Definition	Value
E	Modulus of elasticity of the adherends	1.0E07 psi
υ	Poisson's ratio of the adherends	0.3
E_a	Modulus of elasticity of the adhesive	1.0E06 psi
υ_a	Poisson's ratio of the adhesive	0.3
t	Thickness of the adherends	0.25 in
h	Thickness of the adhesive	0.004 in
c	One half the lap length	1.25 in.
P	Applied force in Figure 3	1000 lb
M_s	Applied moment in Figure 3	1000 lb in
M_b	Applied moment in Figure 3	1000 lb in

In load cases 1 and 2, the adherends are subjected to an axial force, P. In load case 1, reactions are developed to balance the couple caused by P. The vertical reaction forces cause shears at the ends of the adherends. Thus, load case 1 is referred to as Membrane-Shear loading. In load case 2, moments are applied at the ends of the adherends to balance the couple caused by P. The vertical reaction forces, and thus the shear forces at the ends of the adherends, for this case are zero. Thus, this case is referred to as Membrane-Bending loading. So as to examine the full range of possible boundary conditions for the membrane case, load cases 1 and 2 are combined as shown is Figure 4a. In Figure 4a, moments of $-\beta Pt^*/2$ are applied to the ends of the adherends where $t^*=t+h$. Reactions, and thus the amount of shear applied to the ends of the adherends, depend on the parameter,

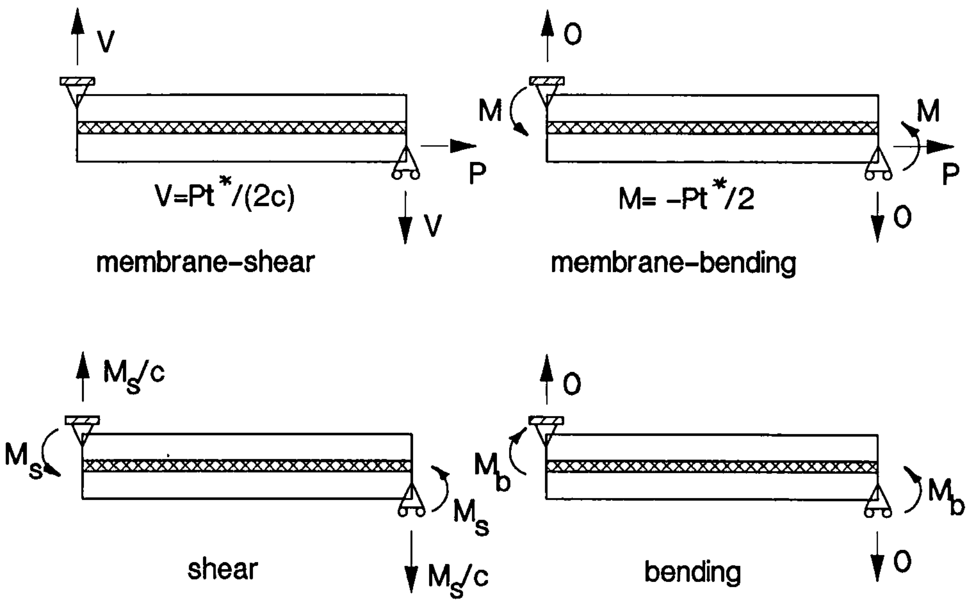

FIGURE 3 Various loadings

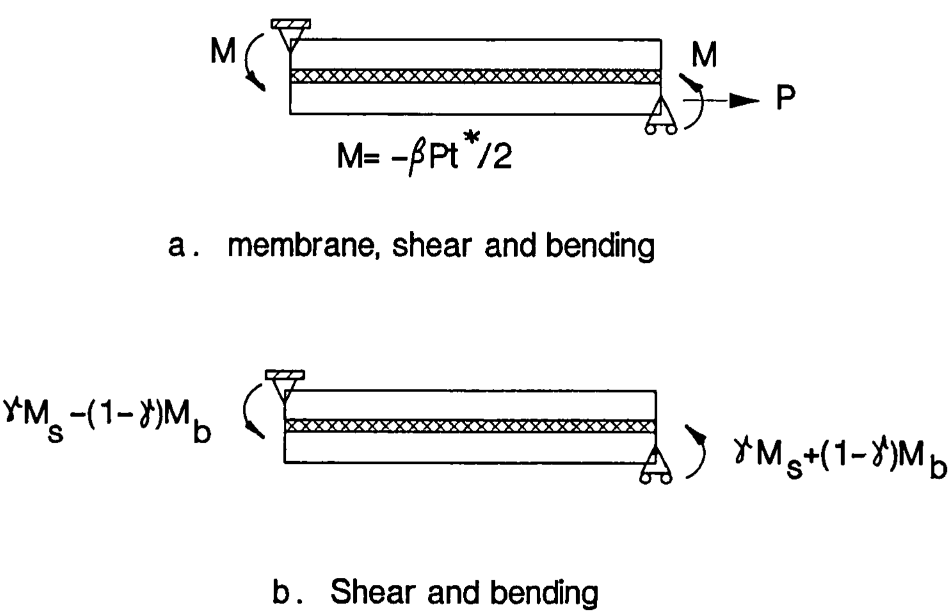

FIGURE 4 Combined loadings

β. When $\beta = 0$, the loading corresponds to the Membrane-Shear loading and when $\beta = 1$, the loading corresponds to the Membrane-Bending loading.

In load case 3, no axial forces are applied to the adherends but moments are applied. These moments cause vertical reaction forces which are shear forces at the ends of the adherends. Thus, this loading is referred to as Shear loading. In load case 4, no axial forces are applied but moments are applied which do not cause vertical reaction forces. Thus, for this loading the shear forces on the adherends are zero, and this loading is referred to as Bending loading. To examine the effects of shear and bending loadings on the adherends in the absence of axial forces, load cases 3 and 4 were combined as shown in Figure 4b. When the parameter $\gamma = 0$ in Figure 4b, the loading corresponds to the Bending loading case and when $\gamma = 1$, the loading corresponds to the Shear loading case.

The joint was analyzed using 100 beam elements for the adherends and 50 special 4-node adhesive elements for the adhesive.[19] A typical beam element is shown in Figures 2 and 5a and a typical 4-node adhesive element is shown in Figures 5a and 5b. The adhesive elements have offset nodes so that they can connect with the beam elements which have their nodes along their centroids as shown in Figure 5a.

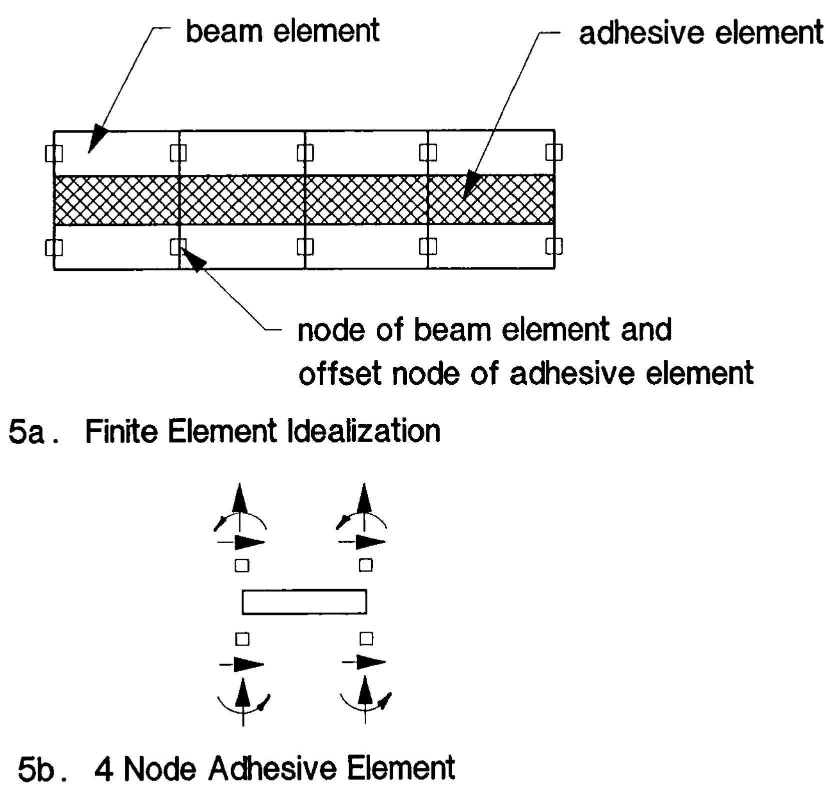

FIGURE 5 Finite element idealization

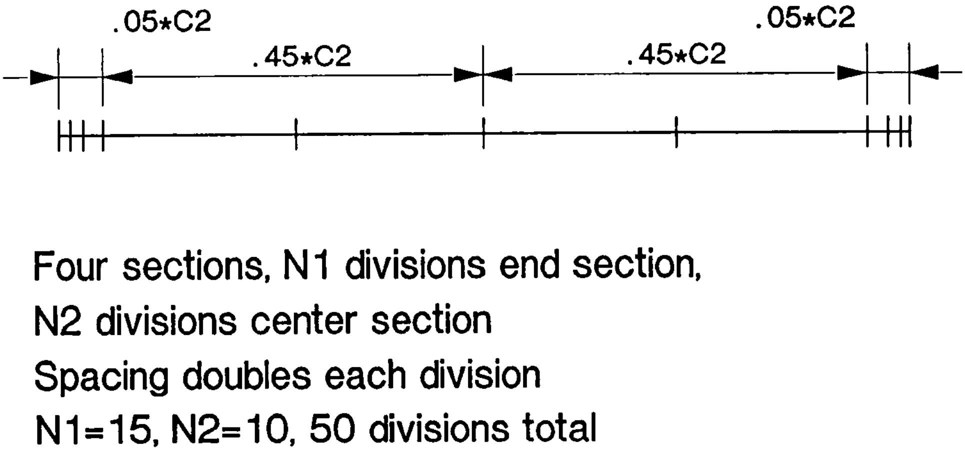

FIGURE 6 Element spacing

Longitudinal spacing of the elements is shown in Figure 6. This arrangement of elements was found to give acceptable convergence of stresses.[19]

For both the Shear-Bending study and the Membrane Shear-Bending study, 10 sets of assumptions were examined. These assumption sets are listed as Cases 1 through 10 in Table III. In Case 1, all parameters are set to 1. In Cases 2–8, all parameters but one are set to 1 while the remaining parameters in turn are set to zero. Case 9 corresponds to the assumptions of Delale and Erdogan.[14] This case was investigated as the theory of Delale and Erdogan is considered one of the best modern day lap joint theories. Case 10 corresponds to the assumptions made by Goland and Reissner[1] in their classic paper.

A typical distribution of adhesive stress along the length of the joint is shown in Figure 7 where the stress is along the top adherend-adhesive interface. The loading for Figure 7 is the Membrane-Shear loading shown in Figure 3 where $P = 1000$ lb.

TABLE III
Control parameters considered

Case	IPLANE	IFIN	α_1	α_2	α_3	α_4	α_5	α_6
1	1	1	1	1	1	1	1	1
2	0	1	1	1	1	1	1	1
3	1	0	1	1	1	1	1	1
4	1	1	0	1	1	1	1	1
5	1	1	1	0	1	1	1	1
6	1	1	1	1	0	1	1	1
7	1	1	1	1	1	0	1	1
8	1	1	1	1	1	1	1	0
9	1	0	0	0	1	1	1	1
10	1	0	0	0	0	0	.743	.910

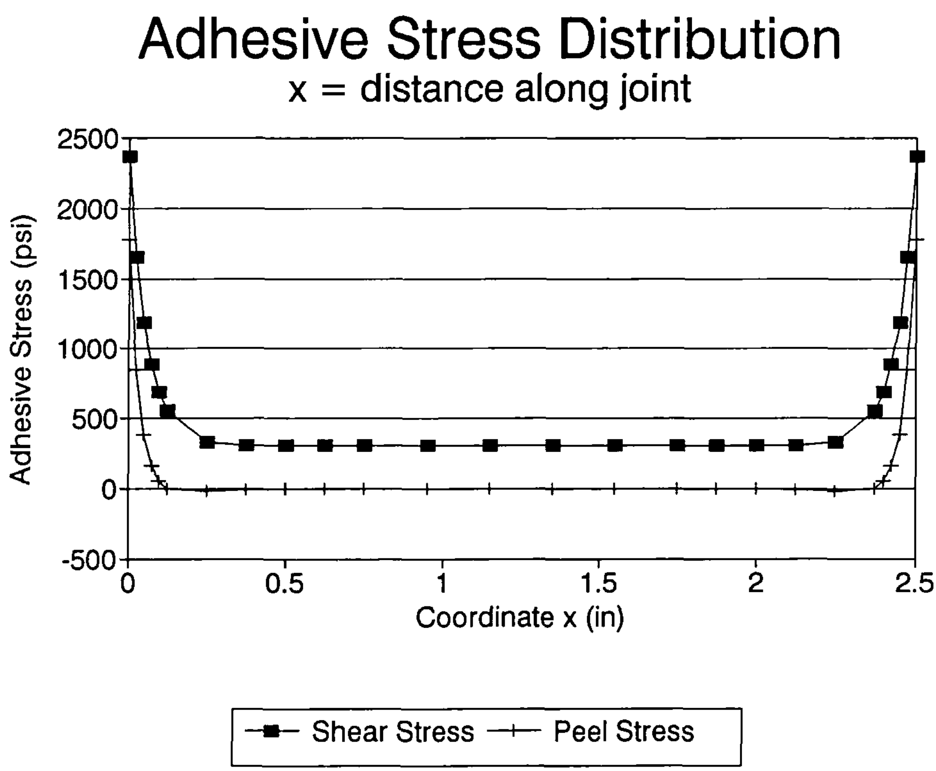

FIGURE 7 Adhesive stress distribution along joint

One can see that maximum adhesive stresses occur at the ends of the joint. It is these maximum stresses which are examined in the following studies.

Figures 8–11 show maximum adhesive normal peel stress (σ_{zz}) and maximum adhesive shear stress. These maximum stresses occur at the edges of the joint. Throughout the examples of this paper, maximum adhesive stresses reported are for the left end of the joint at the top adherend-adhesive interface. Notice that in the Membrane Shear-Bending study as well as in the Shear-Bending study, there was almost no difference in predicted maximum adhesive shear stress for the assumption cases examined.

In both the Membrane Shear-Bending study and the Shear-Bending study, the maximum adhesive peel stress was affected very little by most assumptions. The factors which did affect the maximum adhesive peel stress were:

1. whether plane stress or plane strain was being assumed,
2. whether shear deformation of the adherends was being considered or not, and
3. whether a consistent shear stress-shear strain equation was being employed.

Comparing results with the results of Case 1, the assumption with regard to plane stress or plane strain affected results by approximately 6% while neglecting shear

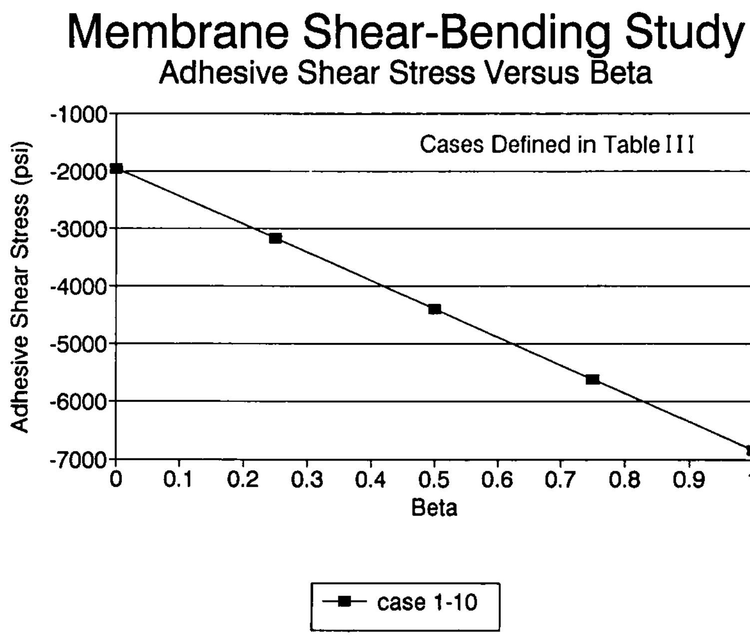

FIGURE 8 Adhesive shear stress, Membrane-Bending Study

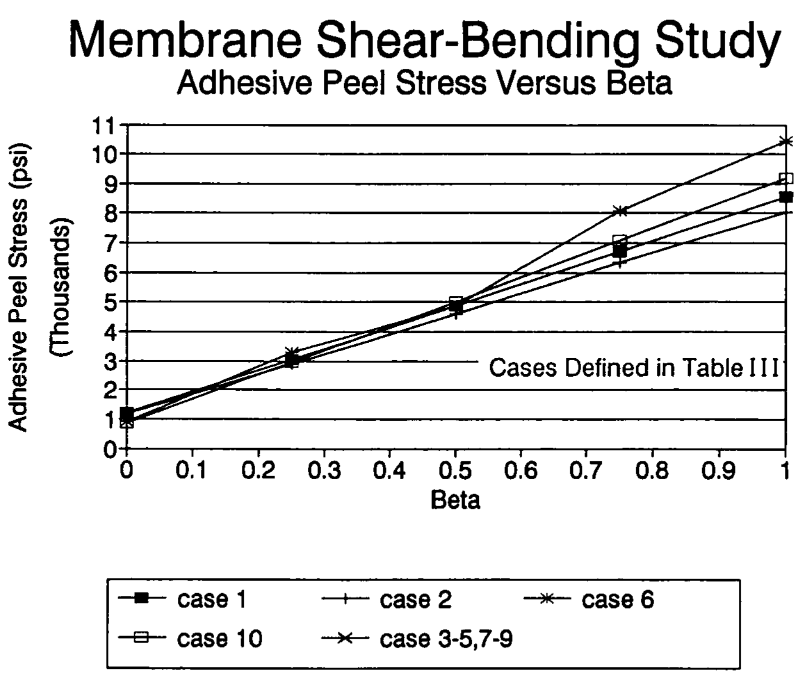

FIGURE 9 Adhesive peel stress, Membrane-Bending Study

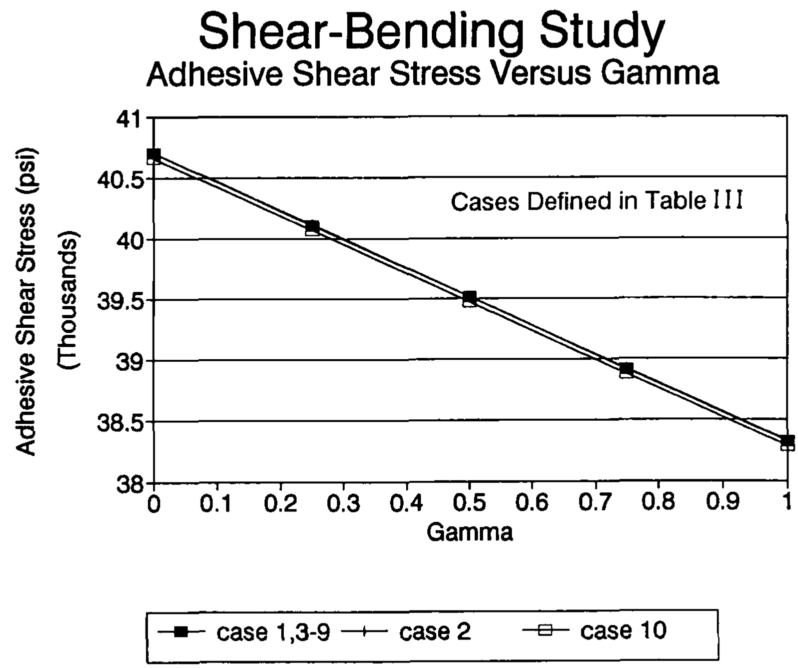

FIGURE 10 Adhesive shear stress, Shear-Bending Study

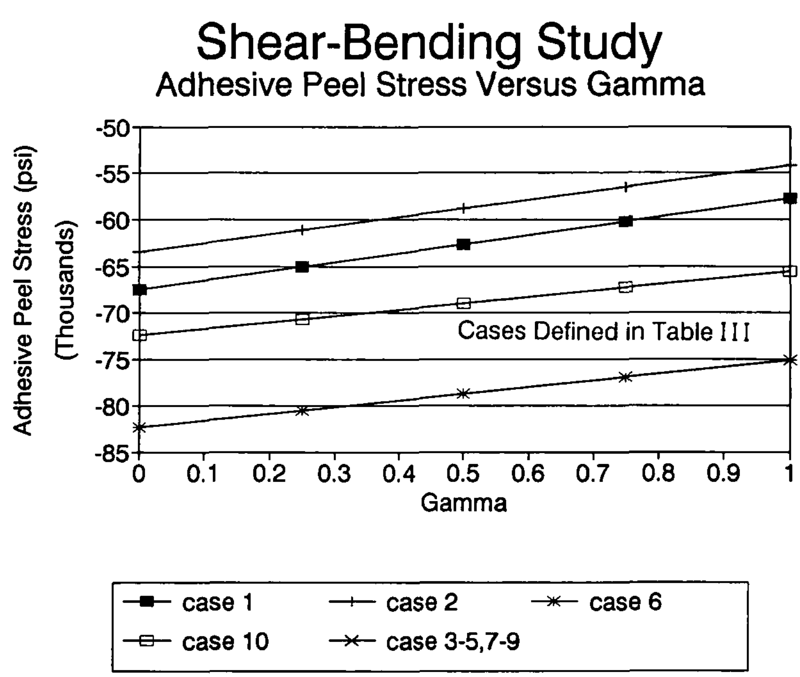

FIGURE 11 Adhesive peel stress, Shear-Bending Study

deformation of the adherends affected results up to 30%. The widely used theory of Goland and Reissner[1] neglects shear deformation of the adherends, inconsistently uses plane stress and plane strain for the adherends, and uses an inconsistent shear stress-shear strain equation for the adhesive. It had a maximum deviation from standard Case 1 of approximately 30% but for most values of β or γ the effects of the inconsistencies cancel the effects of neglecting the shear deformation of the adherends and the deviation was less than 15%.

EXAMPLE 2

The configuration used in this investigation was similar to that of Example 1 with the exception that the modulus of elasticity of the adhesive was varied to yield various E/E_a ratios. Properties of the configuration are given in Table II and the configuration was subjected to Membrane-Shear loading as shown in Figure 3 with $P = 1000$ lb. The ten assumption cases of Table III were investigated. Figure 12 depicts the maximum adhesive shear stress *versus* the parameter E/E_a and Figure 13 depicts the maximum adhesive peel stress *versus* that parameter. As in the previous example, adhesive shear stress can be seen to be insensitive to variations in underlying assumptions. As can be seen in Figure 13, most assumption cases gave approximately the same results with the exception of Cases 6, 10, and 2. In Case 6, the shear deformation of the adherends is being neglected. The maximum adhesive peel stress for this case varied from the standard Case 1 by as much as 27%. Case 10

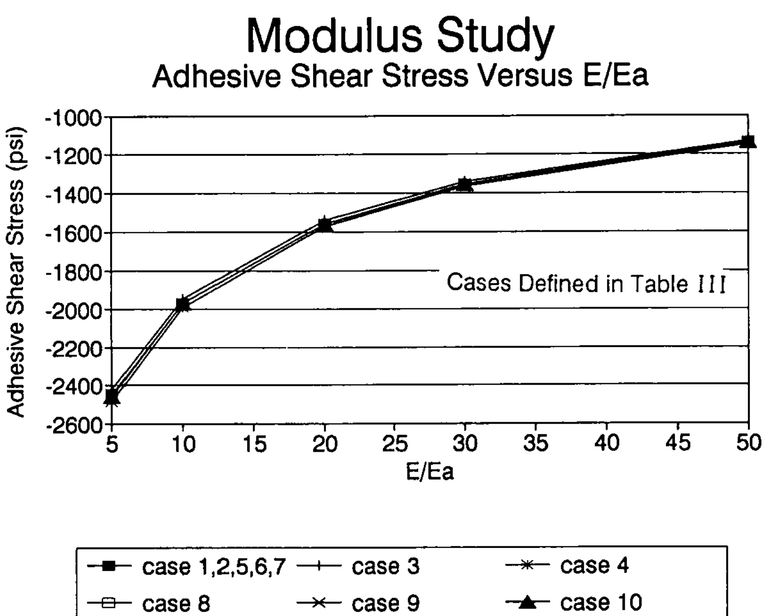

FIGURE 12 Adhesive shear stress, Modulus Study

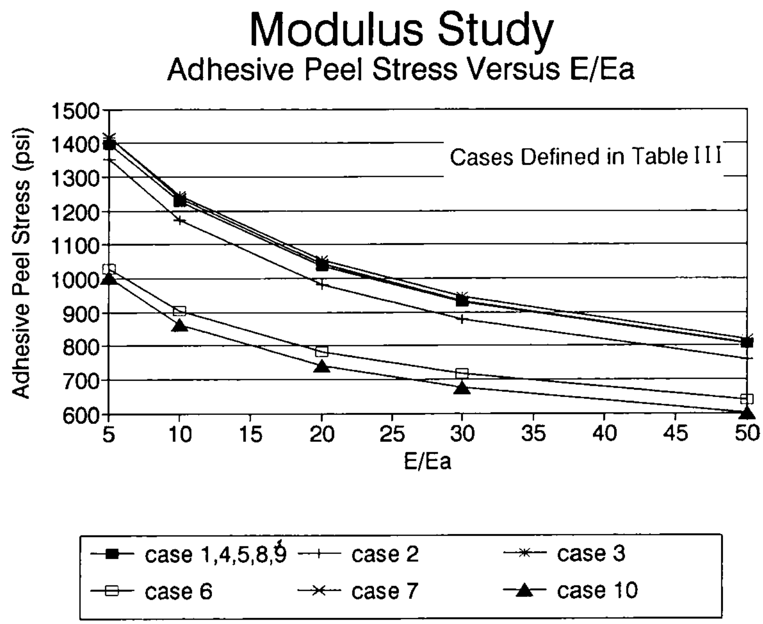

FIGURE 13 Adhesive peel stress, Modulus Study

corresponds to the assumptions of Goland and Reissner[1] where, among other assumptions, the shear deformations of the adherends is neglected. Maximum adhesive peel stress for Case 10 varied from those of standard Case 1 by as much as 29%. Case 2 is the only case where plane stress is being assumed, the other cases assuming plane strain. One can see in Figure 13 that the plane stress assumptions lowered the maximum adhesive peel stress by approximately 5% from standard Case 1.

EXAMPLE 3

Example 3 is similar to Examples 1 and 2 except that in this study the thickness of the adhesive is varied from h = 0.001 in to h = 0.016 in. Properties of the configuration are given in Table II. As in Example 2, the configuration was subjected to Membrane-Shear loading as shown in Figure 3 with P = 1000 lb. Figure 14 depicts the maximum adhesive shear stress *versus* the adhesive thickness and Figure 15 depicts the maximum adhesive peel stress *versus* adhesive thickness. As in the previous two examples, maximum adhesive shear stress can be seen in Figure 14 to be insensitive to the assumption case being considered. Even at the largest adhesive thickness considered, maximum adhesive shear stress, for any of the cases considered, did not vary from standard Case 1 by more than 4%. In Figure 15, one can see that neglecting the shear deformation of the adherend (as in Cases 6 and 10) has the most significant effect on results. The zero adhesive thickness assumption did not affect maximum adhesive peel stress by more than 5%, even for the thickest adhesive examined.

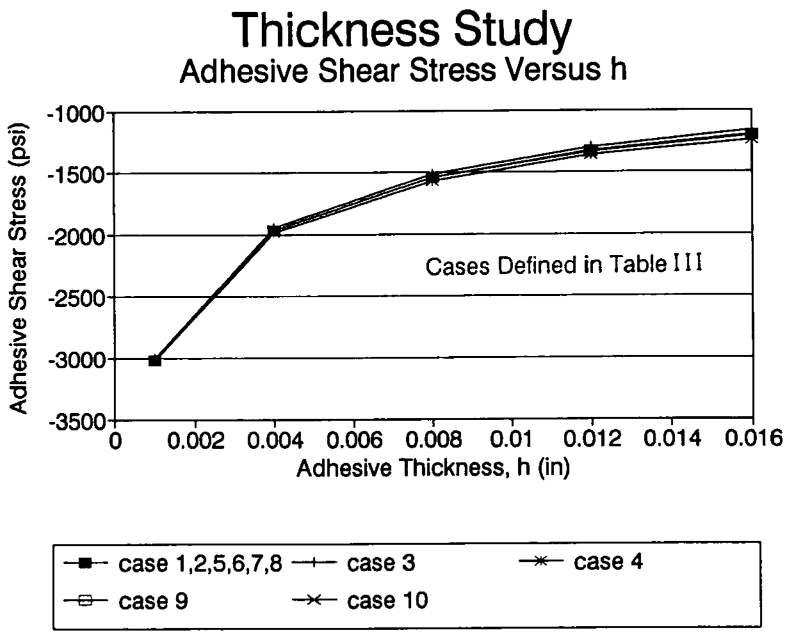

FIGURE 14 Adhesive shear stress, Adhesive Thickness Study

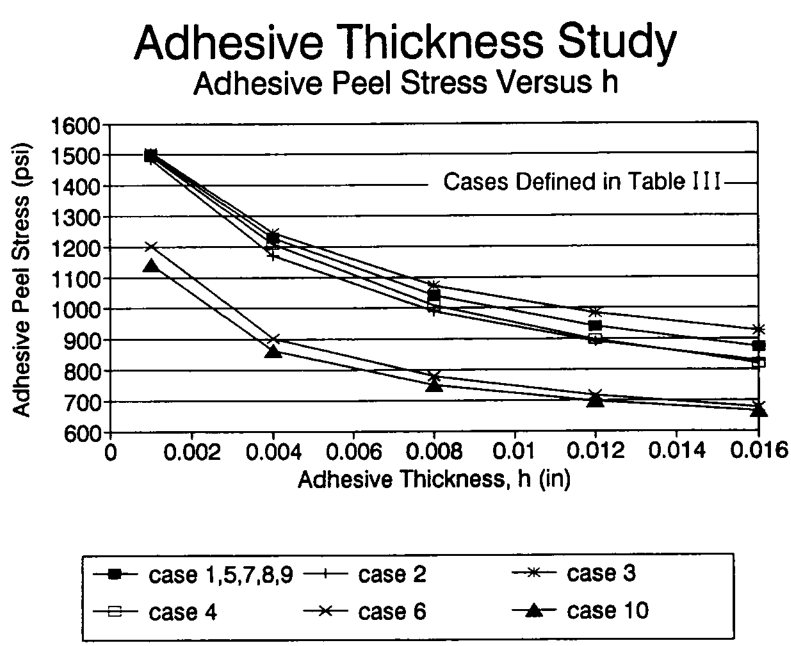

FIGURE 15 Adhesive peel stress, Adhesive Thickness Study

DISCUSSION

This study demonstrates that adhesive stresses obtained from most modern lap joint theories will vary very little from those obtained using the assumptions of Case 1. The special adhesive finite element for Case 1 is nothing but the standard 4-node isoparametric element[21] found in most finite element libraries. Plate or beam elements are also found in most finite element libraries. Thus, this study indicates that the results of lap joint theory can be duplicated with standard elements in readily available finite element programs where the adhesive is modeled with one row of 4-node isoparametric elements. Thus, analysts can conveniently obtain, for arbitrary loads or boundary conditions, results comparable with those obtained with the lap joint theories.

Analysts may be tempted to think that if finite element results using one row of isoparametric elements are comparable with those from lap joint theories, that better results might be obtained using 2, 3 or more rows of adhesive elements. Figure 16 depicts the variation of maximum adhesive shear stress and maximum adhesive peel stresses for the lap joint of Figure 1 with $c=0.625$ in, $t=0.125$ in, $h=0.01$ in, $m=0.75$ in, and $P=1000$ lb and where the adhesive is modeled using the ANSYS[22] finite element program. Each adherend was modeled with 50 beam elements with offset nodes and the adhesive was modeled with varying number of rows of isoparametric elements, each row containing 50 elements. One can see that

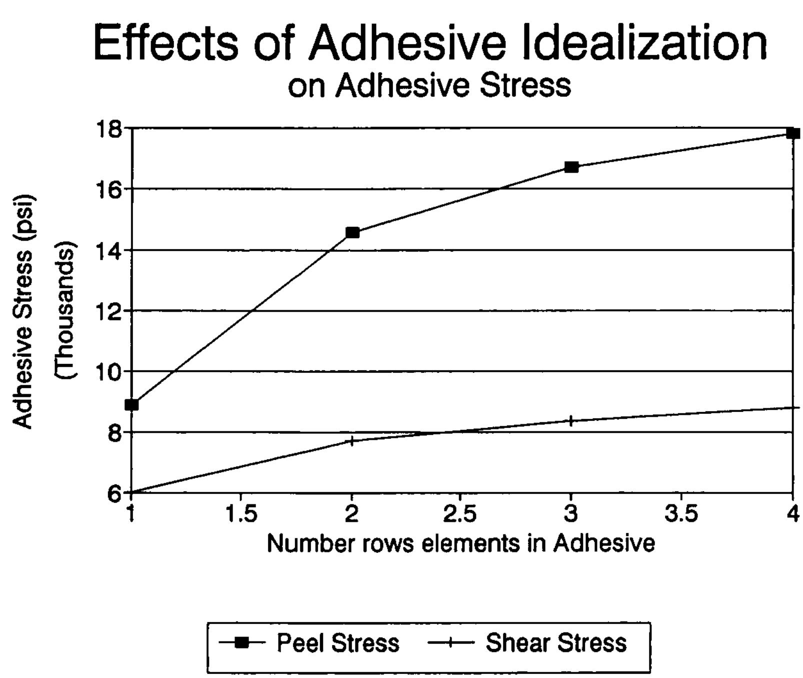

FIGURE 16 Effect of adhesive idealization on adhesive stress

higher values of adhesive stress are obtained as more rows of elements are used to model the adhesive. This increase in stress with refinement of grid reflects the fact that the idealization is coming closer to the exact modeling of the linearized equations of elasticity which predict stress singularities at the corners of the bi-material interfaces.

Stresses obtained from lap joint theories or from finite element idealizations with one row of isoparametric elements modeling the adhesive are artificial values of stress. The reason for using these artificial values is pragmatic. These values are easy to obtain, they alleviate the need to obtain stress intensities from a fracture mechanics analysis, and analysts have almost a half century of experience in using stresses from lap joint theories to predict joint strength. Maximum adhesive stress from finite element analyses with 2 or 3 rows of adhesive elements could be taken as artificial stresses to be used in design. However, these stresses would not correspond to those from the lap joint theories.

CONCLUSION

Over the last several decades, various authors have developed lap joint theories to predict stresses in the adhesive of bonded lap joints. The effect of various assumptions associated with lap joint theories has been studied in this paper. It was found that many of the sundry assumptions made by various authors have insignificant effect on maximum adhesive stress. Several well known theories neglect the effect of shear deformation of the adherends. It was found that neglecting the shear deformation had little effect on adhesive shear stress but could affect the adhesive peel stress by as much as 30%. The classic theory of Goland and Reissner[1] neglects shear deformation of the adherends, inconsistently uses plane stress and plane strain for the adherends, and uses an inconsistent shear stress-shear strain equation for the adhesive. The theory of Goland and Reissner gave adhesive shear stress results that were approximately the same as from theories without those assumptions but the maximum adhesive peel stresses were as much as 30% different. However, in most cases, effects of the inconsistencies cancel the effects of neglecting shear deformation of the adherends and the difference was less than 15%.

It was noted that finite element results, where plate or beam elements were used to model the adherends and one row of 4-node isoparametric elements was used to model the adhesive, were comparable with those obtained from lap joint theories. When 2 or more rows of adhesive elements were used, adhesive stresses were not comparable. This part of the study emphasizes the fact that maximum adhesive stresses from lap joint theories are artificial stresses, which in no way correspond to those obtained from a solution of the linearized equations of elasticity which predict a singular stress state at the corners of the adhesive-adherend interfaces.

References

1. M. Goland and E. Reissner, *J. Appl. Mechanics* **66,** A17–A27 (1944).
2. L. J. Hart-Smith, NASA, Report CR-112234 (1973).
3. T. Wah, *J. Engineering Mat. Technology, ASME* **95,** 174–181 (1973).
4. L. J. Hart-Smith, NASA Report CR-2218 (1974).

5. L. J. Hart-Smith, NASA Report CR-112237 (1973).
6. T. S. Ramamurthy and A. K. Rao, *Int. J. Mech. Sci.* **20,** 721–727 (1978).
7. W. J. Renton and J. R. Vinson, *Air Force Office of Sci. Res.* TR No. 75–0125 (1975).
8. W. J. Renton and J. R. Vinson, *J. Applied Mech.* **44,** 101–106 (1977).
9. G. C. Grimes and L. F. Greiman, *Composite Materials* (Academic Press, New York, 1975), Ch. 10.
10. W. N. Sharpe and T. J. Muha, *Proc. Army on Solid Mechanics* 23–24 (1974).
11. S. Yadagiri, C. Papi Reddy and T. Sanjeeva Reddy, *Computers and Structures* **27,** No. 4, 445–454 (1987).
12. I. U. Ojalvo and H. L. Eidinoff, *AIAA Journal* **16,** 204–211 (1978).
13. Du Chen and Shun Cheng, *J. Appl. Mechanics* **50,** 109–115 (1983).
14. F. Delale and F. Erdogan, *J. Appl. Mechanics* **48,** 331–338 (1981).
15. U. Yuceoglu and D. Updike, *J. Eng. Mech.* **106,** 37 (1980).
16. U. Yuceoglu and D. Updike, *J. Eng. Mech.* **107,** 55 (1981).
17. R. Kline, in *Adhesive Joints,* K. L. Mittal, Ed. (Plenum Press, New York, 1984), p. 587.
18. D. B. Bogy and K. C. Wang, *Int. J. of Solids and Structures* **7,** 993–1005 (1971).
19. W. Carpenter and R. Barsoum, *J. Adhesion* **30,** 25–46 (1989).
20. J. S. Przemieniecki, *Theory of Matrix Structural Analysis* (McGraw Hill, London, 1968), p. 80.
21. O. C. Zienkiewicz and Y. K. Cheung, *The Finite Element Method in Structural and Continuum Mechanics* (McGraw Hill, London, 1967).
22. ANSYS, Engineering Analysis System, Swanson Analysis System, Inc., Houston, Pennsylvania, U.S.A.